Journal for Geometry and Graphics
Volume 23 (2019), No. 1, 99–114.

A Task About Spheres and Cones, Applicable in Jet Theory

Viktor Mileikovskyi

Kyiv National University of Construction and Architecture
Povitroflotskyi pr. 31, room 288, Kyiv, 03037, Ukraine
email: mileikovskyi@gmail.com

Abstract. A task about spheres and cones is solved. The task is about tangent spheres around an x-axis. Three right circular cones with the same apex on the x-axis at $x = 0$ contain corresponding endpoints of diameters of the spheres, perpendicular to x, and centres of the spheres, respectively. Any three adjacent spheres are mutually tangent. Diameters of the spheres are proportional to x. The x-axis intersects all spheres. The goal of the task is to find geometric relations between the involved cones and to give rules for plotting the scheme. The solution allows a transformation of the sphere sequence onto itself by rotation and homothety. In 2D, the right circular cones degenerate to angles formed by two rays starting at the apex, while the cones' axis degenerates to the angle bisector. The spheres degenerate to circles. Therefore, the task has a 2D analogue. If one of the angles is known, the others can be found uniquely. The radii of the circles form a geometric progression. Nevertheless, the 3D task has more freedom. If the opening angle of the largest cone is known, it is possible to find the minimum of the opening angle of the intermediate cone passing through the sphere centres. This task allows a simplified geometric simulation of large eddies in free jets.

Key Words: cone, sphere, tangency, large eddy, jet.

MSC 2010: 51M04, 52C17, 76F40

1. Introduction

There is a lot of tasks about contacting spheres. Most interesting are tasks with practical application. One of the examples is a sphere packing task, which is very important in goods packing, physics etc., [1, 2, 3, 7, 8, 10, 11, 14]. In this work, we will introduce a task about spheres and cones, which is applicable in fluid mechanics, especially in jet theory. Jets contain large-scale growing vortices, which are self-arranged because of geometrical compatibility. The solution of this task provides a discrete model of axis-symmetric (3D) and flat (2D) free jets. It is different from the classical packing tasks because the spheres have different radii, depending on their position.

ISSN 1433-8157/$ 2.50

2. Definition of the task

Let us assume the x-axis starting from a point O (Figure 1a). Let us consider three coaxial right circular cones (hereinafter referred to as "cones") with the same apex O. The cone b (boundary) has the greatest opening angle, the cone s (submerge) has the smallest one, and the cone c (centres) has an intermediate one. There is a sequence of externally tangent spheres, intersecting the x-axis and numbered by $i \in \mathbb{Z}$. The sphere 1 has an arbitrary x-coordinate. The sphere sequence must be infinite in both directions. Any three adjacent spheres ($i-1$, i, and $i+1$) are tangent to each other. The radius R_i of the sphere with no. i is proportional to the x-coordinate x_i of the centre of the sphere with constant of proportionality Θ_R:

$$R_i = \Theta_R \, x_i. \tag{1}$$

The cones s and b contain the respective endpoints S_i and B_i of diameters normal to the x-axis of all spheres. The cone c contains all centres O_i of the spheres. The points of contact between the spheres i and j will be called A_{ij} $(i < j)$.

Let us use a cylindrical coordinate system around the x-axis. A polar axis r starts from the point O and is oriented parallel to the diameter B_1S_1. The angular coordinate φ can be oriented clockwise or counter-clockwise. Both cases provide two identical symmetric solutions; so we will not specify the direction.

The scheme of spheres can be mapped onto itself by appropriate rotations about the x-axis and scalings relatively to the apex O. This condition requires two limitations: the angle difference $|\varphi_{i+1} - \varphi_i|$ between consecutive spheres must be constant (to ensure a coincidence of angular directions of all old and new diameters B_iS_i after the rotation), and the coordinates x_i must form a geometric progression (to ensure scalability). From the two possibilities $\varphi_{i+1} - \varphi_i = \varphi_i - \varphi_{i-1}$ and $\varphi_{i+1} - \varphi_i = -(\varphi_i - \varphi_{i-1})$ we will consider only the first one, which provides uniformity of sphere allocation around the x-axis. The second one can provide the same uniformity only at $\varphi_{i+1} - \varphi_i = \pm\pi$. Both signs provide the same result, so there is no difference if we use the first case.

Alternatively, instead of defining the cone c and the condition above, we can say that the centres of the spheres are on a conical helix around the x-axis with the same opening angle as the cone c. Nevertheless, the sphere 1 has an arbitrary x-coordinate; so the spiral is not fixed. If we change the coordinate freely (which happen in jets), the spiral will rotate forming the cone c (which is very close to the half-velocity surface in jets). For different tasks, it is possible to use both definitions.

As it will be shown, we can introduce the fourth (t) and fifth (u) cones tangent to all spheres. We can restate the task replacing the cones b and s by t and u. This is interesting because it can reduce the task to the packaging one and, possibly, widen the application range. Nevertheless, this causes a more difficult analysis in jets.

It is necessary to figure out the relations (if possible) between the opening angles of the cones. In addition, we need rules for plotting the scheme.

The task has a 2D analogue: A sphere degenerates to a circle in a plane. A right circular cone is a 3D figure that tapers from a circle to a point on the normal to the circle plane, crossing through its centre. In 2D, the cone's axis and the apex do not degrade, but the cone's base can degrade to a line segment normal to the axis. The axis crosses the midpoint of this segment. Thus, a cone degrades to an angle —- two rays, symmetric with respect to the axis, start from the apex.

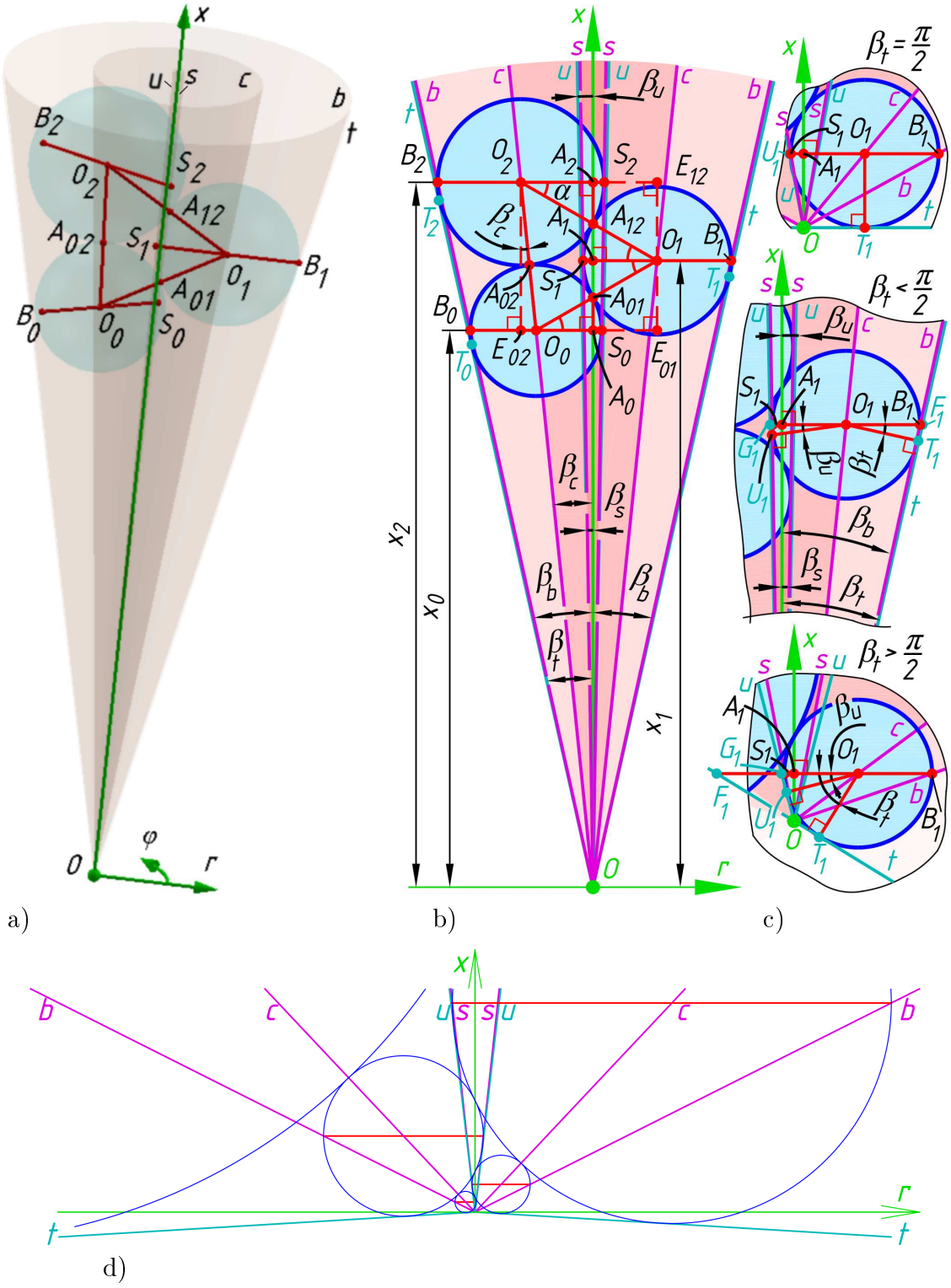

Figure 1: Calculation scheme: a) 3D; b) 2D; c) fragment for solution of the tangent lines t and u; d) example of 2D case at $\Theta_b = 2$ and $\beta_t = (0.518906353122758\ldots)\cdot\pi$

Therefore, the task may be restated from 3D to 2D as follows. Let us assume the x-axis starting from the point O (Figure 1b, c). Let us consider three angles with the same bisector x and vertex O. The angle b (boundary) is the greatest, the angle s (submerge) is the smallest, and the angle c (centres) is intermediate. There is a sequence of tangent circles intersecting

the x-axis. The radius R_i of the circle i is proportional to the x-coordinate (abscissa) x_i of the centre of the sphere by (1). The circle sequence must be infinite in both directions. Any three adjacent spheres ($i-1$, i, and $i+1$) are tangent to each other.

The angles s (the value is $2\beta_s$) and b (the value is $2\beta_b$) contain the respective endpoints S_i and B_i of diameters normal to the x-axis of all circles. The angle c (the value is $2\beta_c$) contains all centres O_i of the circles. The point of contact between the circles i and j ($i < j$) will be called A_{ij}. The points A_i are the intersection points of the diameters B_iS_i and the x-axis.

Remark. No condition of spiral transformation is necessary in this case. We will prove that the transformation is provided by the conditions above (see Corollary 2 hereinafter).

It is necessary to find relations between the angles. In addition, we need rules for plotting the scheme.

3. Limitations

At first, there is a limitation for the 2D and 3D tasks: In both cases, the cones (lines) could be continued in the negative x half-space (half-plane). We will obtain the same picture but in opposite x-direction. Therefore, we will consider only the half-space (half-plane) with positive x. If $\beta_b > \pi/2$, the lines b will pass through the opposite half-plane, relatively to the r-axis. Therefore, the figure at the angles β_b and $\pi - \beta_b$ is the same, and we can restrict the angle to $\beta_b \leq \pi/2$ without losses.

In the case $\beta_b = \pi/2$, the cone (lines) b degenerates to the plane (line) $x = 0$. In the 2D case, the lines A_iB_i coincide with the r-axis, and only two externally tangent circles are possible. In 3D case, the lines A_iB_i are at the plane $x = 0$. The lines should pass through the point O and the point should be inside the spheres. Thus, the point should be a point of contact, and only one pair of spheres can be present at a time. In both cases, the task has no solution.

As a conclusion, there is a limitation, which allows obtaining all possible solutions:

$$\beta_b < \frac{\pi}{2}\,. \tag{2}$$

The limitation allows using tangents of the angles β_b, β_c, and β_s because β_b is the greatest.

Remark. This angle β_t between the tangent line t and the x-axis can be greater than $\pi/2$. The example at $\Theta_b = \tan\beta_b = 2$ has been built using the following calculation results in Figure 1d.

4. 2D solution

At first, the 2D case may be considered: From the circle sequence, let us choose the circle no. 1. The previous circle (closer to the apex O) is no. 0. The next one (farther from apex O) is 2, and so on.

Lemma 1. *All tangency points A_{ij} are located on the x-axis.*

Proof. There is a line $E_{01}E_{12}$ parallel to x crossing the point O_1. The points E_{01} and E_{12} are the intersection points with diameters B_0S_0 and B_2S_2, respectively. As the x-axis is the

bisector of the angle c, the length of the line segments $|O_iA_i|$ is proportional to the respective lengths $|OA_i| = x_{Oi}$ with the proportionality constant $\Theta_c = \tan(\beta_c)$, hence

$$r_{Oi} = |O_iA_i| = \Theta_c\, x. \tag{3}$$

The angle b provides a similar proportionality between the line segments $|OA_i| = x_{Oi}$ and $r_{Bi} = |B_iA_i|$. The corresponding proportionality constant is $\Theta_b = \tan(\beta_b)$, hence

$$r_{Bi} = |B_iA_i| = \Theta_b\, x. \tag{4}$$

Finally, for the angle s there is a proportion between $|OA_i| = x_{Oi}$ and $r_{Si} = |S_iA_i|$ with the proportionality constant $\Theta_s = \tan(\beta_s)$, consequently

$$r_{Si} = |S_iA_i| = \Theta_s\, x. \tag{5}$$

We otain the circle radius $R_i = |O_iB_i| = |B_iS_i| - |O_iS_i| = |O_iS_i| = |O_iA_i| + |S_iA_i|$. Using eqs. (3), (4), and (5),

$$R_i = x_i\,(\Theta_b - \Theta_c) = x_i\,(\Theta_c + \Theta_s)\,. \tag{6}$$

By eqs. (3) and (6) there is a proportion $|O_0A_0|/|O_0A_{01}| = |A_0E_{01}|/|A_{01}O_1|$, because the denominators are the radii. It can be transformed to the following proportion:

$$\frac{|O_0A_0|}{|O_0A_{01}|} = \frac{|O_0E_{01}|}{|O_0O_1|}.$$

By the SAS theorem, $\triangle A_0O_0A_{01} \sim \triangle E_{01}O_0O_1$. Thus, $A_{01}A_0 \perp O_0E_{01}$. Since $A_{01}A_0 \perp x$ and x crosses the point A_0, the line $A_{01}A_0$ is collinear with the x-axis. Therefore, all tangency points A_{ij} are on the x-axis, which was to be proved. □

The following right-angled triangles are also similar: $\triangle A_0O_0A_{01} \sim \triangle A_2O_2A_{12}$, because of proportional radii and distances from the centres to the x-axis (hypotenuse-leg similarity). Thus, $|O_0A_0|/|O_0A_{01}| = |O_2A_2|/|O_2A_{12}|$. Therefore, using the acute angle similarity,

$$\triangle O_0E_{01}O_1 \sim \triangle O_0A_0A_{01} \sim \triangle O_1A_1A_{01} = \triangle O_1A_1A_{12} \sim \triangle O_2A_2A_{12} \sim \triangle O_2E_{12}O_1. \tag{7}$$

Lemma 2. *There is a scaling factor, with which scaling or mirroring in the x-axis and scaling with respect to the centre O, converts Figure 1b onto itself.*

Proof. It is possible to define a system of equations that allows obtaining Figure 1b for different values of parameters. In [9], there was a first attempt to solve the task. It was very simplified, believing without proof, that $A_{01} \in x$, and skipping some of the following equations "by analogy", which cause oversimplified assumptions.

From the right-angled triangle $\triangle O_0A_0A_{01}$, using (3) and (4),

$$\cos\alpha = \cos\angle\, A_0O_0A_{01} = \frac{r_{O0}}{R_0} = \frac{\Theta_c}{\Theta_b - \Theta_c}. \tag{8}$$

From the right-angled triangle $\triangle O_0E_{01}O_1$ we obtain

$$R_0 + R_1 = \frac{x_1 - x_0}{\sin\alpha}. \tag{9}$$

Using eqs. (1), (3), and (4) and introducing the relative x-coordinate as

$$\tilde{x}_i = \frac{x_i}{x_1}, \tag{10}$$

we can transform (9) as follows:

$$(\tilde{x}_0 + 1)\,(\Theta_b - \Theta_c) = \frac{1 - \tilde{x}_0}{\sin\alpha}. \tag{11}$$

From the right-angled triangle $\triangle O_2 E_{12} O_1$ we obtain

$$R_1 + R_2 = \frac{x_2 - x_1}{\sin\alpha}. \tag{12}$$

Using eqs. (1), (3), (4), and (10), we can transform (9) as follows:

$$(1 + \tilde{x}_2)\,(\Theta_b - \Theta_c) = \frac{\tilde{x}_2 - 1}{\sin\alpha}. \tag{13}$$

The equations (11) and (13) are very similar, but the third "analogous" equation with $\tilde{x}_0$ and $\tilde{x}_2$ is the oversimplified assumption of [9]. The third equation can be written from the right triangle $\triangle O_2 E_{02} O_0$, where $O_2 E_{02}$ is the perpendicular from the point O_2 to the line $O_0 S_0$. Therefore, $O_2 E_{02} \parallel x$, and the angle $\angle E_{02} O_2 O_0 = \beta_c$. Thus,

$$R_0 + R_2 = \frac{x_2 - x_0}{\cos\beta_c}. \tag{14}$$

Using eqs. (1), (3), (4), and (10), we can transform (14) as follows:

$$(\tilde{x}_0 + \tilde{x}_2)\,(\Theta_b - \Theta_c) = \frac{\tilde{x}_2 - \tilde{x}_0}{\cos\beta_c} = (\tilde{x}_2 - \tilde{x}_0)\sqrt{1 + \Theta_c^2}\,. \tag{15}$$

Let us eliminate the sine from eqs. (11) and (13):

$$\frac{1 - \tilde{x}_0}{1 + \tilde{x}_0} = \frac{\tilde{x}_2 - 1}{\tilde{x}_2 + 1}. \tag{16}$$

After transformations of (16) it is possible to obtain the very important property of the relative x-coordinates of the circle centres,

$$\tilde{x}_0 = \frac{1}{\tilde{x}_2}. \tag{17}$$

Equation (17) with (10) shows that the x-coordinates of the centres of the circles form a geometric progression with the denominator $\tilde{x}_2$. Scaling (or mirroring in the x-axis and scaling) with the centre O converts Figure 1b into itself at the factors $\tilde{x}_2^n$ for $n \in \mathbb{Z}$. □

Corollary 1. *The sequence of circles is infinite in both directions toward the x-axis and approaching the point O.*

Corollary 2. *All circles can be obtained from a single one by a spiral transformation, that is the product of rotation about the x-axis through the angle π and a scaling with the factor $\tilde{x}_2$ with respect to the centre O: $R_j = R_i \tilde{x}_2^{j-i}$, $x_j = x_i \tilde{x}_2^{j-i}$, $r_{Oj} = x_{Oi} \tilde{x}_2^{j-i}$ for $i \in \mathbb{Z}$ and $j \in \mathbb{Z}$.*

The substitution of (17) to (18) and a simple transformation give the following:

$$\tilde{x}_{0,2} = \sqrt{\frac{\sqrt{1+\Theta_c^2} \mp (\Theta_b - \Theta_c)}{\sqrt{1+\Theta_c^2} \pm (\Theta_b - \Theta_c)}} = \sqrt{1 \mp \frac{2}{\frac{\sqrt{1+\Theta_c^2}}{\Theta_b - \Theta_c} \pm 1}}. \tag{18}$$

The top sign is for x_0 and the bottom one is for $\tilde{x}_2 = x_{i+1}/x_i$, the common ratio of the geometric progression x_i. It is real if

$$1 \mp \frac{2}{\frac{\sqrt{1+\Theta_c^2}}{\Theta_b - \Theta_c} \pm 1} \geq 0. \tag{19}$$

The inequality (19) is equivalent to

$$\Theta_c > \frac{\Theta_b^2 - 1}{2\Theta_b}. \tag{20}$$

Substituting (8) into (11) and using the condition $x_2 > 1$, we obtain

$$(\tilde{x}_2 + 1)^2 (\Theta_b - \Theta_c)^2 \left[1 - \left(\frac{\Theta_c}{\Theta_b - \Theta_c}\right)^2\right] - (\tilde{x}_2 - 1)^2 = 0. \tag{21}$$

Equation (21) can have a solution only if the expression in square brackets is positive, so

$$\Theta_c < \frac{\Theta_b}{2}. \tag{22}$$

From the inequalities (20) and (22) the root isolating interval of Θ_c is

$$\max\left(0, \frac{\Theta_b^2 - 1}{2\Theta_b}\right) < \Theta_c < \frac{\Theta_b}{2}. \tag{23}$$

Substitution of (18) to (21) gives a single, but cumbersome, equation. For the numerical solution, the better option is the same numerical substitution.

In addition, we can connect the tangents Θ_b, Θ_c and the parameters Θ_R using the line A_iB_i, which consists of the circle i radius O_iB_i and the distance $|O_1A_1|$ between the circle centre and the x-axis:

$$\Theta_R = \Theta_b - \Theta_c. \tag{24}$$

From (6) and (24) it is possible to find the tangent of the half-angle s as

$$\Theta_s = \Theta_b - 2\Theta_c = \Theta_R - \Theta_c. \tag{25}$$

The equation (21), after substitution of (18), has been solved in the range (23), divided by 1000 sections, using SciLab (Figure 2). The results can be approximated in the range $\Theta_b \leq 6$ ($\beta_b \leq 80.53\,^\circ$) with relative tolerance up to 0.0089 % (at least four correct significant digits):

$$\begin{aligned} \Theta_c/\Theta_b = {} & -6.153\,10^{-6}\,\Theta_b^5 + 0.0001395\,\Theta_b^4 - 0.001206\,\Theta_b^3 + 0.004367\,\Theta_b^2 - 0.000584\,\Theta_b \\ & + 0.46414, \end{aligned} \tag{26}$$

$$\begin{aligned} \tilde{x}_2 = {} & -7.17\,10^{-6}\,\Theta_b^6 + 0.000162\,\Theta_b^5 - 0.0017656\,\Theta_b^4 + 0.014628\,\Theta_b^3 + 0.1461\,\Theta_b^2 \\ & + 0.53486\,\Theta_b + 1.00006. \end{aligned} \tag{27}$$

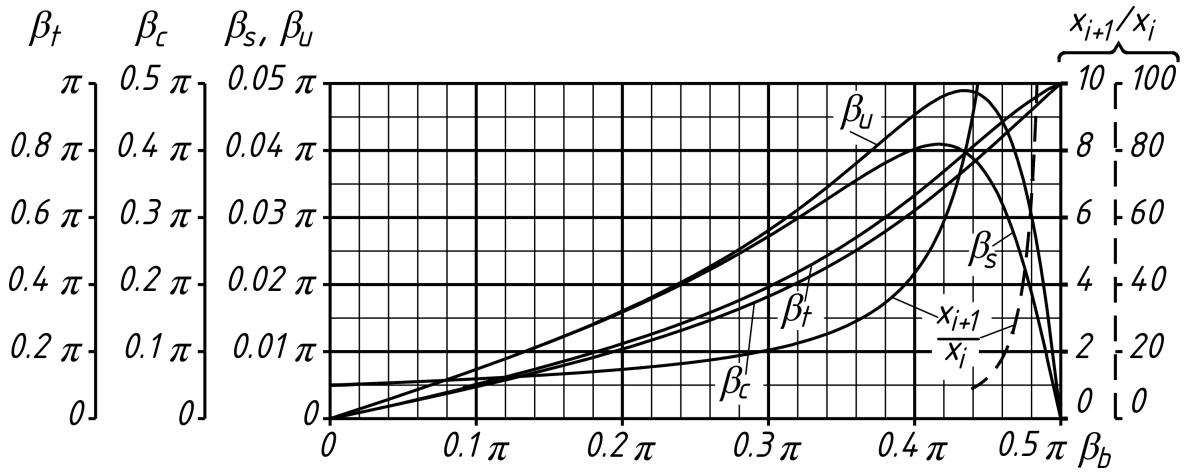

Figure 2: The tangents and the common ratio in the 2D case and in the 3D case for $\varphi_{i+1} - \varphi_i = \pi$

For the jet simulation, this range is very large and (26) is too difficult. In engineering calculations the following approximation is enough for the shorter range $\Theta_b \le 3$ ($\beta_b \le 71,57\,^\circ$) with the same relative tolerance — up to 0.0087 % (at least four correct significant digits):

$$\Theta_c/\Theta_b = -0.00051327\,\Theta_b^3 + 0.0031463\,\Theta_b^2 - 0.000115\,\Theta_b + 0.464087 \tag{28}$$

$$\tilde{x}_2 = -0.000911\,\Theta_b^4 + 0.0129692\,\Theta_b^3 + 0.14729\,\Theta_b^2 + 0.5346274\,\Theta_b + 1.000063. \tag{29}$$

The most important value is $\Theta_b = 0.22$, which corresponds to free jets. In this case, $\Theta_c = 0.1021$ and $\Theta_s = 0.01573$. The first result deviates from [9] only by 0.3 %. Therefore, the simplifications in [9] are not critical. Thus, all results obtained in the author's works have enough precision for engineering calculations and scientific researches.

Finally, we can reduce the task to the packaging one. Let us introduce lines t (external) and u (internal) from the point O tangent to the circles 0 and 1. As other circles can be obtained from them by homothetic transformation with the centre O, the lines are tangent to all circles. The angle between the x-axis and the line t is β_t with the tangent Θ_t. The angle between the x-axis and the line u is β_u, and the tangent Θ_u. The angle γ between the lines c and t is equal to the angle between c and u,

$$\beta_t - \beta_c = \beta_c + \beta_u.$$

After applying the tangent to both sides and after simple transformations, we obtain

$$\Theta_u = \frac{\Theta_t - \Theta_c\,(2 + \Theta_c\Theta_t)}{1 + \Theta_c\,(2\Theta_t - \Theta_c)}, \quad \Theta_u\left(\beta_t = \frac{\pi}{2}\right) = \lim_{\Theta_t \to \infty} \Theta_u = \frac{1 - \Theta_c^2}{2\Theta_c}. \tag{30}$$

Let us draw a perpendicular O_1T_1 from the point O_1 to the line t. The length of it is the radius of the circle 1. Using (6),

$$|O_1T_1| = R_1 = x_1(\Theta_b - \Theta_c). \tag{31}$$

One important characteristic case is $\beta_t = \pi/2$. As the line t is normal to the x-axis, the perpendicular $|O_1T_1|$ is parallel to x-axis. Therefore, $R_1 = x_1$ and, by (31), $\Theta_b - \Theta_c = 1$.

Substituting the result to eqs. (18) and (21) allows an analytical solution. From (25) and (30) follows

$$\tilde{x}_2 = \frac{3+\sqrt{5}}{2} = 2.61803\ldots, \quad \tilde{x}_0 = \frac{3-\sqrt{5}}{2} = 0.381966\ldots, \quad \Theta_b = \frac{5+2\sqrt{5}}{5} = 1.894427\ldots,$$
$$\Theta_c = \frac{2\sqrt{5}}{5} = 0.894427\ldots, \quad \Theta_s = \frac{5-2\sqrt{5}}{5} = 0.1055728\ldots, \quad \Theta_u = \frac{\sqrt{5}}{20} = 0.111803\ldots$$

In other cases, extending the line $|O_1B_1|$ to the line t, gives a point F_1. The length of the line O_1F_1 is

$$|O_1F_1| = |A_1F_1| \mp |A_1O_1| = x_1\left(\pm\Theta_t \mp \Theta_c\right) = x_1\left|\Theta_t - \Theta_c\right|, \tag{32}$$

where the top signs hold for $\beta_t < \pi/2$, the bottom signs for $\beta_t > \pi/2$. From the right-angled triangle $\triangle O_1T_1F_1$, in which $\angle T_1O_1B_1 = \beta_t$ due to perpendicular sides, follows

$$\Theta_b - \Theta_c = \left|\Theta_t - \Theta_c\right|\cos\beta_t = \frac{\left|\Theta_t - \Theta_c\right|}{\sqrt{\Theta_t^2+1}}. \tag{33}$$

There is the solution of (33):

$$\Theta_t = \frac{\Theta_c \pm \sqrt{\Theta_c^2 + \Theta_b\left(1-\left(\Theta_b-\Theta_c\right)^2\right)\left(\Theta_b-2\Theta_c\right)}}{1-\left(\Theta_b-\Theta_c\right)^2}. \tag{34}$$

Analogically, we can find the angle β_u between the x-axis and the line u. From the centre O_1 we should put a perpendicular O_1U_1 to the line u that is tangent to the circle 1. In addition, we should extend the line O_1S_1 to the line u. The new endpoint is G_1. The new triangle $\triangle O_1U_1G_1$ has the right angle $O_1U_1G_1$ and the angle $U_1O_1G_1$ is equal to β_u. Using (6), the leg is

$$|O_1U_1| = R_1 = x_1(\Theta_b - \Theta_c) = x_1(\Theta_s + \Theta_c) \tag{35}$$

and the hypotenuse

$$|O_1G_1| = x_1\left(\Theta_u + \Theta_c\right). \tag{36}$$

From the triangle follows

$$\Theta_b - \Theta_c = \Theta_s + \Theta_c = \left(\Theta_u + \Theta_c\right)\cos\beta_u = \frac{\Theta_u + \Theta_c}{\sqrt{\Theta_u^2+1}}, \tag{37}$$

$$\Theta_u = \frac{-\Theta_c \mp \sqrt{\Theta_c^2 + \Theta_b\left(1-\left(\Theta_b-\Theta_c\right)^2\right)\left(\Theta_b-2\Theta_c\right)}}{1-\left(\Theta_b-\Theta_c\right)^2} \tag{38}$$

Equations (34) and (38) have only one positive value at $\Theta_b - \Theta_c < 1$ ($\beta_t < \pi/2$). It corresponds to the plus sign. Both equations at $\Theta_b - \Theta_c > 1$ ($\beta_t > \pi/2$) have two solutions: the solutions of (34) are negative, the solutions of (38) are positive, which corresponds to the geometric meaning. The most important peculiarity is the same absolute value of the solutions at the top signs, as well as at the bottom signs. Thus, we should accept the solution with greater absolute value and negative sign as Θ_t and with lower absolute value as Θ_u. Therefore, there are universal equations, which can be transformed using (24),

$$\Theta_t = \frac{\sqrt{\Theta_c^2 + \Theta_b\left(1-\left(\Theta_b-\Theta_c\right)^2\right)\left(\Theta_b-2\Theta_c\right)} + \Theta_c}{1-\left(\Theta_b-\Theta_c\right)^2} = \frac{\sqrt{\Theta_c^2 + \left(1-\Theta_R^2\right)\left(\Theta_R^2-\Theta_c^2\right)} + \Theta_c}{1-\Theta_R^2}. \tag{39}$$

$$\Theta_u = \frac{\sqrt{\Theta_c^2 + \Theta_b\left(1-\left(\Theta_b-\Theta_c\right)^2\right)\left(\Theta_b-2\Theta_c\right)} - \Theta_c}{1-\left(\Theta_b-\Theta_c\right)^2} = \frac{\sqrt{\Theta_c^2 + \left(1-\Theta_R^2\right)\left(\Theta_R^2-\Theta_c^2\right)} - \Theta_c}{1-\Theta_R^2}. \tag{40}$$

Thus, we solved the 2D task.

- The relation between the characteristic angles can be found from (21) after substitution of (18) in the root isolation interval (23) at known Θ_b or Θ_c. In addition, eqs. (39) and (40) give a possibility to calculate the tangent lines. For engineering calculations, we can use the eqs. (26) or (28), instead.
- The spheres can be built by the sequence of the x- and r-coordinates of their centres and their radii. The denominator $\tilde{x}_2$ of the progression of x-coordinates should be found by (18). For engineering calculations, the approximations (27) of (29) can be used, instead. After that, we should put a coordinate x_1 and compute the x-coordinates progression as $x_i = x_1 \tilde{x}_2^{i-1}$, the corresponding radii by (1) and the r-coordinates by (3).

The examples are displayed in Figure 1b and d.

5. 3D solution

After the 2D solution, we will solve the 3D task. From the sequence of spheres, let us choose a sphere no. 1. The previous sphere (closer to the apex O) is 0, the next one (farther from the apex O) is 2, and so on.

The polar coordinate of i-th sphere centre (on the cone c) is proportional to its x-coordinate by (3), where Θ_c is the tangent of half of the opening angle (angle between some generatrix of the cone c and the x-axis). The equations (3) and (4) are also valid. Therefore, for the definition of some spheres, it is enough to set only two coordinates of its centre O_i: x_i and φ_i. Let us assume that x_1 is known. We may set $\varphi_1 = 0$.

The tangency between spheres will define the other. The tangency between the spheres i and j ($|j - i| \leq 2$) says that the distance between the sphere centres is equal to the sum of their radii, $|O_i O_j| = R_i + R_j$, or

$$\sqrt{(x_j - x_i)^2 + (r_j \cos(\varphi_j) - r_i \cos(\varphi_i))^2 + (r_j \sin(\varphi_j) - r_i \sin(\varphi_i))^2} = R_i + R_j. \qquad (41)$$

After the substitution of eqs. (1), (3), and (10) and simple transformations, (41) is equivalent to

$$\frac{\tilde{\Delta}_{ij}}{\tilde{x}_i} = \sqrt{\left(\frac{\tilde{x}_j}{\tilde{x}_i} - 1\right)^2 + \Theta_c^2 \left(\left(\frac{\tilde{x}_j}{\tilde{x}_i}\right)^2 + 1 - 2\frac{\tilde{x}_j}{\tilde{x}_i}\cos(\varphi_j - \varphi_i)\right)} - \Theta_R \left(\frac{\tilde{x}_j}{\tilde{x}_i} + 1\right) = 0. \qquad (42)$$

The absolute value of $\tilde{\Delta}_{ij}$ equals the distance between the closest points of non-overlapping spheres (if $\tilde{\Delta}_{ij} > 0$) or the most deeply overlapped points of overlapping spheres (if $\tilde{\Delta}_{ij} < 0$), that corresponds to x_1.

Dividing both parts of (42) by $\tilde{x}_j/\tilde{x}_i$ gives the same equation as replacing $\tilde{x}_j/\tilde{x}_i$ by $\tilde{x}_i/\tilde{x}_j$. Therefore, if a value of $\tilde{x}_j/\tilde{x}_i$ is a root, the reciprocal value is also a root.

Equation (10) implies $\tilde{x}_1 = 1$. Thus, from (42) at $j = 1$,

$$\tilde{\Delta}_{i1} = \sqrt{(\tilde{x}_i - 1)^2 + \Theta_c^2 (\tilde{x}_i^2 + 1 - 2\tilde{x}_i \cos(\varphi_i))} - \Theta_R (\tilde{x}_i + 1) = 0. \qquad (43)$$

Both eqs. (42) and (43) have non-negative radicands. The first members of the radicands are squares of expressions. At the greatest possible value of cosine, namely 1, the second

members are also squares of expressions. As the coordinates $\tilde{x}_i$ and $\tilde{x}_j$ can be only non-negative, a smaller cosine value causes not a smaller value of the second members. Thus both members are non-negative.

The cosine from (42) and (43) satisfies

$$-1 \le \cos(\varphi_j - \varphi_i) = \frac{\left(\frac{\tilde{x}_j}{\tilde{x}_i} - 1\right)^2 + \Theta_c^2\left(\left(\frac{\tilde{x}_j}{\tilde{x}_i}\right)^2 + 1\right) - \Theta_R^2\left(\frac{\tilde{x}_j}{\tilde{x}_i} + 1\right)^2}{2\Theta_c^2\,\frac{\tilde{x}_j}{\tilde{x}_i}} \le 1. \tag{44}$$

Three spheres 0, 1 and 2 give two identical equations (43) and one equation (42). There are four unknowns — two relative coordinates and two angles. Thus, there are multiple solutions with one degree of freedom. The geometric progression of x_i or the constant angle difference $\varphi_i - \varphi_{i-1}$ can fully define the problem. Both conditions are equivalent by (44).

Using the geometric progression condition, the equations can be solved easily. (43) has two solutions for the tangency of the spheres 1 and 2 and the spheres 0 and 1, respectively:

$$\tilde{x}_2 = \frac{\sqrt{\left(2\Theta_R^2 - \Theta_c^2(1-\cos(\varphi_2))\right)\left(\Theta_c^2(\cos(\varphi_2)+1)+2\right)} + \Theta_c^2\cos(\varphi_2) + \Theta_R^2 + 1}{\Theta_c^2 - \Theta_R^2 + 1} \ge 1, \tag{45}$$

$$\tilde{x}_0 = \frac{1}{\tilde{x}_2}. \tag{46}$$

For the spheres 0 and 2, (42) should be applied using

$$\frac{\tilde{x}_j}{\tilde{x}_i} = \frac{\tilde{x}_{i+2}}{\tilde{x}_i} = \tilde{x}_2^2 \quad \text{and } \varphi_j - \varphi_i = \varphi_{i+2} - \varphi_i = 2\varphi_2. \tag{47}$$

The solution > 1 of (42), using (47), is

$$\tilde{x}_2 = \sqrt{\frac{\sqrt{\left(2\Theta_R^2 - \Theta_c^2(1-\cos(2\varphi_2))\right)\left(\Theta_c^2(\cos(2\varphi_2)+1)+2\right)} + \Theta_c^2\cos(2\varphi_2) + \Theta_R^2 + 1}{\Theta_c^2 - \Theta_R^2 + 1}}. \tag{48}$$

The eqs. (45) and (48) give a single equation for the angle step φ_2:

$$\begin{aligned}\left(\sqrt{\left(2\Theta_R^2 - \Theta_c^2(1-\cos\varphi_2)\right)\left(\Theta_c^2(\cos\varphi_2+1)+2\right)} + \Theta_c^2\cos\varphi_2 + \Theta_R^2 + 1\right)^2 &= \left(\Theta_c^2 - \Theta_R^2 + 1\right) \\ \times \left(2\sqrt{\left(\Theta_R^2 - \Theta_c^2(1-\cos^2\varphi_2)\right)\left(\Theta_c^2\cos^2\varphi_2 + 1\right) + \Theta_c^2(2\cos^2\varphi_2 - 1) + \Theta_R^2 + 1}\right).\end{aligned} \tag{49}$$

The equation (49) has been symbolically solved, which is very easy using Maxima algebra system. After getting rid of the roots (two times), the equation will be quartic. Its depressed equation is biquadratic, but it has only two different second order roots,

$$\cos\varphi_2 = \frac{\pm\Theta_R\sqrt{2\left(\Theta_R^2+3\right)\left(1-\Theta_R^2+\Theta_c^2\right)} + \left(\Theta_R^2+1\right)\Theta_c}{\left(1-\Theta_R^2\right)\Theta_c}. \tag{50}$$

We choose the real solution in the range $[-1, 1]$.

Let us discuss the most characteristic cases of the task. To find the minimum possible value of Θ_c, let us differentiate (44) by Θ_c:

$$\frac{d\cos(\varphi_j - \varphi_i)}{d\Theta_c} = \frac{\left(\Theta_R + 1 + \frac{\tilde{x}_j}{\tilde{x}_i}\left((\Theta_R - 1)\right)\right)\left(\Theta_R - 1 + \frac{\tilde{x}_j}{\tilde{x}_i}(\Theta_R + 1)\right)}{\Theta_c^3\,\frac{\tilde{x}_j}{\tilde{x}_i}}. \tag{51}$$

The derivative has only one discontinuity at $\tilde{x}_j/\tilde{x}_i = 0$ and two non-positive roots at $\Theta_R \leq 1$:

$$\frac{\tilde{x}_j}{\tilde{x}_i} = \frac{\Theta_R \pm 1}{\Theta_R \mp 1}. \tag{52}$$

The derivative cannot change its sign at $\tilde{x}_j/\tilde{x}_i > 0$. At $\tilde{x}_j/\tilde{x}_i = 1$, the derivative (51) is $4\Theta_R^2/\Theta_c^3 > 0$. Thus, the derivative is positive, so the function is increasing. The minimum possible value of Θ_c is corresponding to the minimum possible value of cosine — minus one. The angle is π; so all sphere centres and tangency points are in the same plane. The intersection with the plane is the same as in Figure 1b. Moreover, the results of the 2D task incl. Figure 2, (26), (27), (28), and (29) are acceptable. Four spheres cannot be tangent to each other. To check the solution, a function in SciLab has been created. The function tests the possibility of a solution at $\Theta_c = \Theta_R$ (always) and at $\Theta_c = 0$ (never). The minimum point of Θ_c with the last possible solution can be found by the bisection method. Calculations show that at the minimum $|\varphi_0| = |\varphi_2| = \pi$.

The next characteristic case is $\Theta_c \to \Theta_R = \Theta_b/2$. It is the special case, which allows four tangent spheres: two pairs of opposite ones. The lines between the centres of the pairs are perpendicular. However, if Θ_c is infinitely less than $\Theta_b/2$, only three spheres (by numeric solution) can be tangent each other. The numeric solution (Figure 3) can be approximated by the following equations of the common ratio and angular coordinate difference in radians between adjacent spheres with the respective deviations 0.012 % and 0.0025 %:

$$x_{i+1}/x_i = -0.00237\,\Theta_b^3 + 0.07273\,\Theta_b^2 + 0.36394\,\Theta_b + 1.00011, \tag{53}$$

$$\varphi_{i+1} - \varphi_i = -0.000773\,\Theta_b^4 + 0.0008082\,\Theta_b^3 + 0.0687363\,\Theta_b^2 + 0.3654873\,\Theta_b + 1.000024. \tag{54}$$

The third characteristic case is the average value of Θ_c between the first and the second characteristic cases (Figure 4). The following approximation has the respective deviations

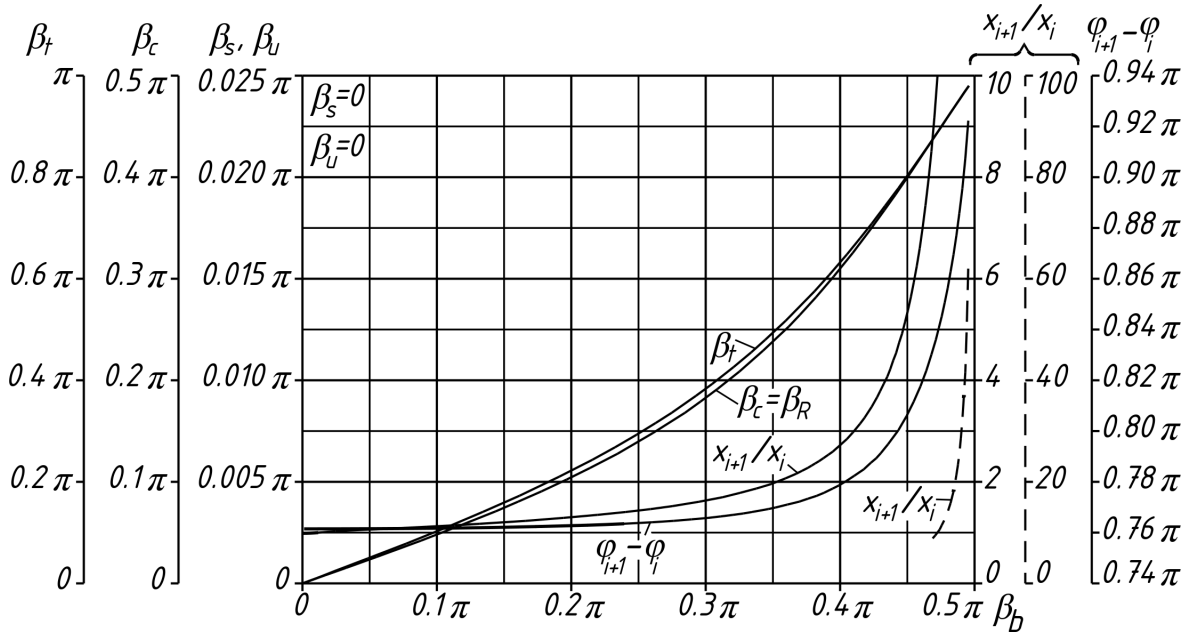

Figure 3: The angle difference, the tangents, and the common ratio in the 3D case if $\Theta_c = \Theta_R$

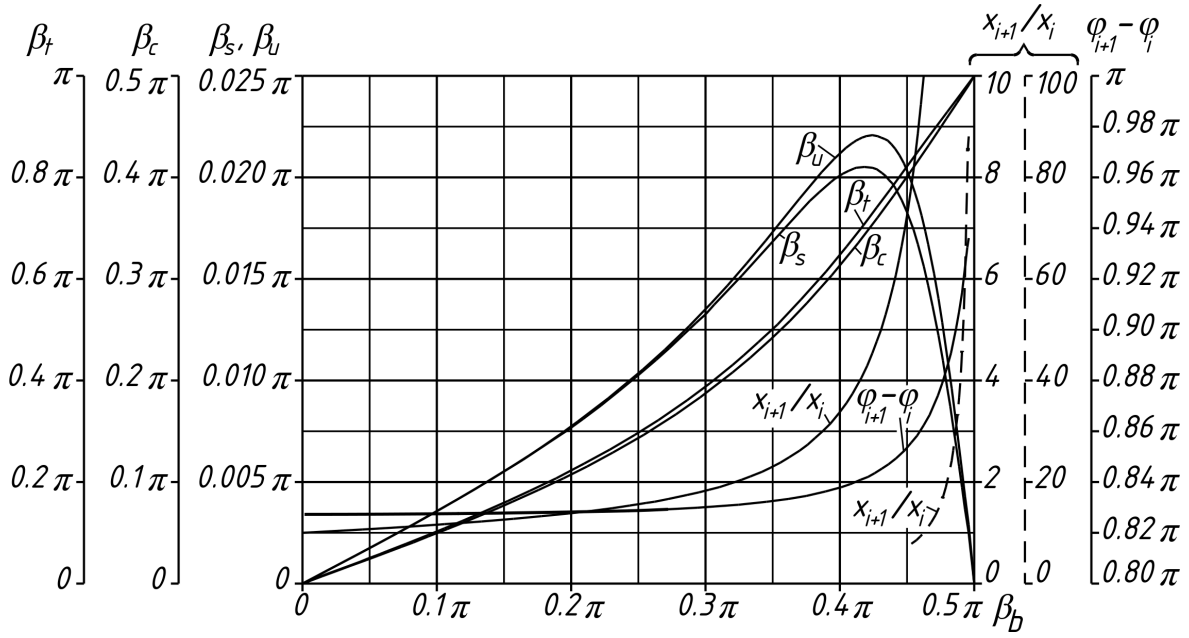

Figure 4: The angle difference, the tangents, and the common ratio in the 3D case at the average value of Θ_c

0.0058 %, 0.008 %, 0.0064 %, and 0.002 %:

$$\Theta_c/\Theta_b = -0.000216\,\Theta_b^3 + 0.00141\,\Theta_b^2 + 0.482692, \tag{55}$$

$$\Theta_s/\Theta_b = -0.00004\,\Theta_b^5 + 0.0002364\,\Theta_b^4 - 0.0025905\,\Theta_b^2 + 0.0346523, \tag{56}$$

$$\varphi_{i+1} - \varphi_i = 0.0036\,\Theta_b^2 + 0.00139\,\Theta_b + 2.598875; \tag{57}$$

$$x_{i+1}/x_i = -0.00201\,\Theta_b^4 + 0.00633\,\Theta_b^3 + 0.103668\,\Theta_b^2 + 0.45301\,\Theta_b + 1.000019. \tag{58}$$

In other cases it is necessary to solve the equations. For a crude approximation, it is possible to calculate the parameters at the three cases above and perform a parabolic interpolation.

For the cone t, which is tangent to all spheres externally, and the cone u, which is tangent to all spheres internally, eqs. (39) and (40) are applicable. Let us build a plane through the x-axis and the centre of the sphere 1. The intersection of the cones and the sphere 1 with this plane is the same as Figure 1c. Thus, the development of the equations in the 2D case is applicable to the 3D case.

Thus, we solved the 3D task.

- The relation between the characteristic angles is not fixed. At first, we should assume the tangent Θ_b of the cone b. The tangent of the cone c should be accepted in the range $\Theta_c = [\Theta_{c,\min},\, \Theta_b/2]$, where the minimum value $\Theta_{c,\min}$ is the same as in the 2D task by eqs. (18) and (21) in the root isolation interval (23). Alternatively, we can assume Θ_c. After that, Θ_b should be accepted inside the range $\Theta_b = [2\Theta_c,\, \Theta_{b,\max}]$, where the maximum value $\Theta_{b,\max}$ is the same as in the 2D task by the same equations. Other tangents can be found from eqs. (25), (39), and (40).
- The spheres can be built by the geometric progressions of the x- and r-coordinates of centres and the radii, and also by the step of the angle φ. The denominator $\tilde{x}_2$

of progression of the x-coordinates and the angle step φ can be found by (51) and (45). For engineering calculations, the approximations (27), (29), (53), (54), (55), (56), (57), and (58) can be used instead for the corresponding cases. In other cases, we can interpolate the approximation results. After that, we should define a coordinate x_1 and compute the x-coordinate progression $x_i = x_1 \tilde{x}_2^{i-1}$, the corresponding radii by (1), and the r-coordinates by (3).

An example is shown in Figure 1a.

6. Application of the results

The presented solution gives a discrete jet model, which can be used for the simulation of ventilation airflows for the development of energy-efficient air exchange organization in rooms [4]. One of the most important problems is energy efficiency. During the euro-integration process [6] Ukraine highly increases the energy efficiency of constructions. Airflows in rooms (both averaged and turbulent parameters) are a very important part [4, 12] in the energy efficiency of ventilation. Air jets have a large-scale vorticity, which allows the simulation of the macrostructure using the presented method. At a low Reynolds number, the macrostructure is visible [5, 15] in dyed jets (Figure 5) and very similar to Figure 1a. The cones represent the characteristic jet dimensions: jet boundary, half-velocity surface and interaction deepness between vortices. As there is no difference in the equations for jet parameters in ventilation, we can extend the macrostructure analysis on the wide range of Reynolds numbers.

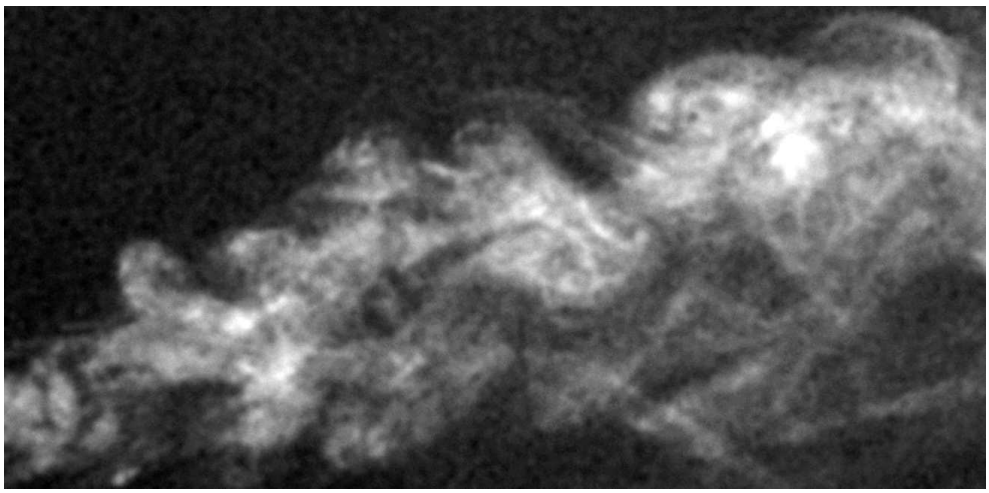

Figure 5: A free jet, dyed by uranine

A new direction of rising the energy efficiency of buildings by airflows with turbulent macrostructure is the control of the "cooling effect" of "green structures" [13], which are structures of buildings with living plants. The plants cool air and structures by evaporation, which is dependent on air velocity and turbulence intensity. A specially designed parapet of "green goofs" can control the airflows for maximizing the "cooling effect" only in summer for passive air conditioning. The simulation method is used for optimization of the parapet.

7. Conclusions

The solution of the 2D task about angles and tangent circles was found. It required a numeric solution of an equation. In addition, the solution of the 3D task about spheres and cones was found. The 3D case adds up to the 2D one in extreme cases — lowest opening angle of the cone with the sphere centres. The tasks can simply represent the macrostructure of free jet flows in hydro-aerodynamics.

8. Prospects for further research

The simulation of air velocity and turbulence intensity of 3D jets using the model is finished. A successful optimization of air distributors with multiple tangential slots using the simulation method shows its usability. Now we are focused on the optimization of air exchange in rooms.

Acknowledgments

The authors thanks the professor of the Heat Gas Supply and Ventilation Department of Kyiv National University of Construction and Architecture, Andrei Tkachuk (1928–2002), for the foundation of this research direction in the university.

References

[1] P. Chaikin: *Random Thoughts*. Physics today **60**/6, 8–9 (2007).

[2] S. Chaoming, W. Ping, H.F. Makse: *A phase diagram for jammed matter*. Nature **453**, 629–632 (2008).

[3] Z. Chuanming: *From deep holes to free planes*. Bull. Amer. Math. Soc. **39**, 533–555 (2002).

[4] V. Dovhaliuk, V. Mileikovskyi: *New approach for refined efficiency estimation of air exchange organization*. Internat. J. Eng. Technol. **7]/(3.2)**, 591–596 (2018).

[5] O. Gumen, V. Dovhaliuk, V. Mileikovskyi: *Simplified simulation of flows with turbulent macrostructure*. Hydraulic Engineering IV – Proceedings of the 4th Internat. Technical Conference on Hydraulic Engineering, CHE 2016, Hong-Kong, pp. 251–260.

[6] O. Gumen, N. Spodyniuk, M. Ulewicz, Y. Martyn: *Research of Thermal Processes in Industrial Premises with Energy-Saving Technologies of Heating*. Diagnostyka **18**/2, 43–49 (2017).

[7] D. de Laat, F. de Oliveira, M. Fernando, F. Vallentin: *Upper bounds for packings of spheres of several radii*. Forum of Mathematics, Sigma **2**, e23, 42 p. (2014).

[8] G.W. Marshall, T.S. Hudson: *Dense binary sphere packings*. Beitr. Algebra Geom. **51**/2, 337–344 (2010).

[9] V. Milejkovskyi: *Geometrical Modelling of the jet boundary layer*. 25th National and 2nd International Scientific Conference moNGeometrija 2010, Belgrade/Serbia, pp. 352–362.

[10] P.I. O'Toole, T.S. Hudson: *New High-Density Packings of Similarly Sized Binary Spheres*. J. Phys. Chem. **115**/39, 19037–19040 (2011).

[11] D.L. Rosen: *Random thoughts on densest packing*. Physics today **61**/4, 12 (2008).

[12] N. Spodyniuk, V. Zhelykh, O. Dzeryn: *Combined heating systems of premises for breeding of young pigs and poultry.* FME Transactions **46**, 651–657 (2018).

[13] T. Tkachenko: *Energy efficiency of "green structures" in cooling period.* Internat. J. Eng. Technol. **7**/(3.2), 453–457 (2018).

[14] S. Torquato, F.H. Stillinger: *Toward the jamming threshold of sphere packings: Tunneled crystals.* J. Appl. Phys. **102**, 093511 (2007).

[15] Y.S. Tsai, J.C.R. Hunt, F.T.M. Nieuwstadt, J. Westerweel, B.P.N. Gunasekaran: *Effect of Strong External Turbulence on a Wall Jet Boundary Layer.* Flow Turbulence Combust. **79**, 155–174 (2007).

Received May 8, 2018; final form February 25, 2019